리튬 금속 전극상 고분자/무기물 나노복합막 형성:
리튬층의 효과적 표면성장 제어 및 전기화학적 특성 향상

정 요 한*·석 도 형*·이 상 현*·신 원 호**·손 희 상*,†

*광운대학교 화학공학과, **광운대학교 전자재료공학과
(2020년 1월 15일 접수, 2020년 1월 23일 수정, 2020년 1월 27일 채택)

Polymer/Inorganic Nanohybrid Membrane on Lithium Metal Electrode:
Effective Control of Surficial Growth of Lithium Layer and Its Improved Electrochemical Performance

Yohan Jeong*, Dohyeong Seok*, Sanghyun Lee*, Weon Ho Shin**, and Hiesang Sohn*,†

*Department of Chemical Engineering, Kwangwoon University, Seoul 01897, Republic of Korea
**Department of Electronic Material Engineering, Kwangwoon University, Seoul 01897, Republic of Korea
(Received January 15, 2020, Revised January 23, 2020, Accepted January 27, 2020)

요   약: 리튬 덴드라이트의 효과적인 억제를 위해 유/무기 복합체를 리튬메탈 전극의 보호층으로 사용하였다. 유기물로는 PVDF-HFP가 사용되었으며 무기물로는 TiO_2가 사용되었다. 유기물로 사용된 PVDF-HFP는 높은 유연성을 가지는 고분자로서 무기물의 matrix 역할을 하며, 무기물로 사용된 TiO_2 나노입자는 보호막의 기계적 강도와 이온전도성을 향상시켜주는 역할을 하였다. 합성된 보호막은 SEM, AFM, XRD를 통하여 PVDF-HFP matrix에 TiO_2가 잘 분산되어 있는 형태인 것을 확인할 수 있었다. 또한 전기화학적 분석 결과, 향상된 기계적 물성과 이온전도성으로 인해 polymer-inorganic composite은 비교 샘플(untreated 와 PVDF-HFP 보호층) 대비 100번째 사이클까지 80%의 높은 쿨롱 효율 및 20 mV 미만의 낮은 과전압을 나타내었다.

Abstract: Polymer/inorganic composites were used as a protective layer of lihitum metal electrode for effective suppression of lithium dendrite. PVDF-HFP was used as an polymer material and TiO_2 nanoparticle was used as an inorganic material. PVDF-HFP is a highly flexible polymer that acts as a matrix of inorganic materials while TiO_2 nanoparticle improves the mechanical strength and ion conductivity of the protective layer. The as-synthesized protective hybrid membrane exhibited good dispersion of TiO_2 in the PVDF-HFP matrix by SEM, AFM and XRD analyses. Furthermore, the electrochemical analysis showed that the polymer-inorganic composite retained high coulombic efficiency of 80% and low overpotential, less than 20 mV until the 100th cycles due to the improved mechanical properties and ion conductivity in comparison to the control sample (untreated and PVDF-HFP polymers/Cu).

Keywords: *lithium metal battery, lithium dendirte, polymer/inorganic hybrid, PVDF-HFP, TiO₂*

1. Introduction

As energy consumption increases, the demand of high capacity, high energy density energy storage devices has also been increasing[1-3]. Accordingly, researches on rechargeable secondary batteries are performed a lot.

Lithium ion batteries have been most widely commercialized due to their high voltage, low self discharge, stable cycling and wide operating temperature range[4-6]. However, lithium ion batteries are expensive and have the disadvantage of low energy density[7-10]. In order to solve the problem of lithium ion batteries, researches

†Corresponding author(e-mail: hsohn@kw.ac.kr, http://orcid.org/0000-0002-4164-9397)

on lithium metal batteries have been actively conducted, which use lithium metal (3,860 mAh/g) as an anode material instead of graphite anode because graphite based anode has a low theoretical capacity (372 mAh/g) [11,12]. Lithium metal electrode forms a solid electrolyte interface (SEI) layer on the surface of the lithium metal by an interfacial reaction between lithium metal and electrolyte during charging/discharging reaction. At this time, a non-uniformly SEI layer is formed and exhibits relatively low resistance or defective parts. Also, lithium dendrite is formed by intensive lithium redox reactions in which lithium grows vertically, and the lithium dendrite generates dead lithium after repeated cycles, which shortens the life span of the battery. In addition, lithium dendrite can growth through the separator and cause internal short circuits, which can also affect safety issues such as battery explosion[13].

There are two ways to suppress the growth of lithium dendrite. Firstly, uniform deposition of lithium is available using lithiophilic materials before lithium dendrite growth at the nucleation step. Secondly, it is required to design a protective layer that can mechanically suppress lithium dendrite on the lithium electrode. The protective layer is mainly composed of polymers. Among them, PVDF-HFP has been studied as a gel-type polymer electrolyte due to its high flexibility, chemical and physical stability, good compatibility with electrodes and ion conductivity. In addition, inorganic TiO_2 can not only increase the ion conductivity of the polymer matrix through Lewis acid-base interaction with the polymer or lithium salt anion, but also improve the mechanical properties of the protective layer thanks to the high mechanical strength of the inorganic material [14-16].

In this study, a composite of PVDF-HFP and TiO_2 (PVDF-HFP@TiO_2 membrane) was designed as a protective layer of lithium metal for effective suppression of lithium dendrite. The designed protective layer was found to effectively inhibit lithium dendrite by improved ion conductivity and mechanical properties.

2. Experimental

2.1. Materials and reagents

Interfacial synthesis was applied to synthesize nano-sized TiO_2 particles. Titanium isopropoxide (TTIP, Sigma-Aldrich, 97%) was used as a precursor. Oleic acid (Daejung, Extra pure), tert-butylamine (Duksan, Extra pure), toluene (Samchun, 99.5%) were used as the solvent to be used in the interfacial synthesis method. Polyvinlyidene fluoride-co-hexafluoropropylene, (PDVF-HFP, Sigma-Aldrich) was used as a polymer, and N-methyl-2-pyrrolidone (NMP, Sigma-Aldrich) was used as solvent to dissolve polymer and nanoparticle precursors.

2.2. Material syntheses
2.2.1. Synthesis of precursor

In a typical synthesis, 0.1 mL of tert-butylamine was dissolved in 10 mL of water and the solution was transferred to a 50 mL Telfon-lined stainless-steel autoclave. Subsequently, 3 g of titanium isopropoxide and 10 g of oleic acid were dissolved in 60 mL of toluene and the solution was transferred to the autoclave. The autoclave was maintained at 180°C for 8 h and cooled to room temperature. The solution of TiO_2 was precipitated using methanol and centrifugation. The synthesized TiO_2 particles and PVDF-HFP were put in NMP and the dispersion was well performed. TiO_2 content was varied (0~5 wt%) before mixing it with PVDF-HFP coating precursor.

2.2.2. Deposition of hybrid film

As-prepared coating precursors were deposited on Cu substrate with a blade coater at 30 μm and dried for 4 h at 50°C in an oven. Subsequently, an electrochemical Li|Cu half-cell was fabricated using PVDF-HFP/TiO_2 hybrid membrane on Cu substrate in a glove box. Then, lithium layer was formed between Cu and PVDF-HFP/TiO_2 hybrid membrane via electrochemical deposition method.
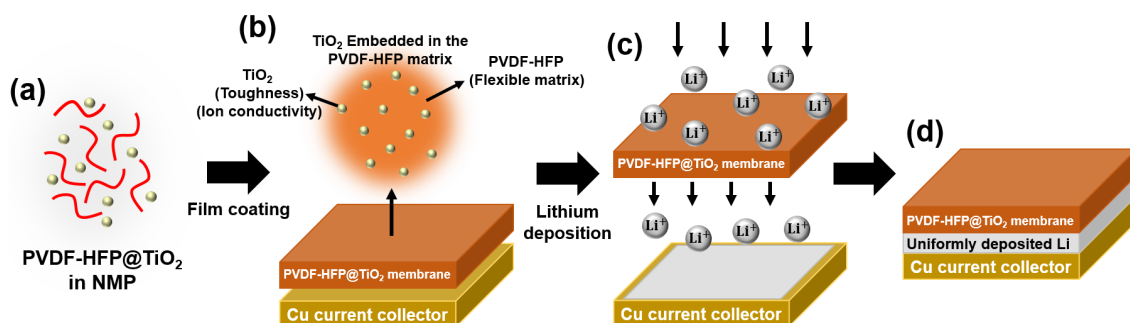
Scheme 1. (a) Preparation of coating solution. (b) Structure of PVDF-HFP@TiO$_2$ hybrid membrane. (c) Lithium deposition on coated Cu electrode. (d) Uniformly deposited Li metal electrode between PVDF-HFP@TiO$_2$ hybrid membrane and Cu electrode.

2.3. Material characterizations

To confirm that the design proceeded as intended, we analyzed the presence of TiO$_2$ in the polymer and analyzed the electrochemical properties of the designed hybrid membrane. The morphology and elemental distribution of the surface of PVDF-HFP/TiO$_2$ hybrid membrane was observed by scanning electron microscope (SEM) and energy dispersive X-ray spectroscopy (EDS) to identify the elements in TiO$_2$ and PVDF-HFP. Atomic force microscope (AFM) was performed to observe the surface morphology of PVDF-HFP/TiO$_2$ hybrid membrane.

2.4. Electrochemical characterizations

For electrochemical characterization, CR-2032-Type coin half cell was fabricated using lithium as a counter electrode and PVDF-HFP/TiO$_2$ hybrid membrane coated Cu electrode as a working electrode. Electrolyte contained 1 M of LiTFSI in 1,3-dioxolane (DOL)/ 1,2-dimethoxyethane (DME) (1 : 1 = v : v). Coin cells were fabricated in a glove box filled with argon. Coulombic efficiency, voltage profiles, and voltage-time curves were measured by battery tester. Initial cycles were plated to a capacity of 3 mAh/cm^2 with a current density of 0.1 mA/cm^2 for uniform deposition of lithium and stripped of lithium to 1.2 V. Electrochemical impedance spectroscopy (EIS) was measured in the frequency range from 100 kHz to 0.1 Hz using a potentiostat.

3. Results and Discussion

3.1. Design of PVDF-HFP@TiO$_2$ hybrid membrane

Scheme 1 shows the fabrication process of the PVDF-HFP@TiO$_2$ hybrid membrane, the structure of protective layer and the lithium deposition characteristics. In the preparation of the coating solution, PVDF-HFP is first dissolved in NMP, and then TiO$_2$ nanoparticles obtained by solvothermal synthesis are added to the prepared solution with different mass compositions [Scheme 1(a)]. After sufficiently stirring the PVDF-HFP and TiO$_2$ nanoparticles to be evenly mixed, coating on the Cu current collector is performed by blade coating technic. The coated film has a structure in which TiO$_2$ nanoparticles are well dispersed in PVDF-HFP polymer matrix [Scheme 1(b)]. Coin cell is manufactured using the coated Cu electrode. Lithium is deposited on the coated Cu electrode by using electrical deposition [Scheme 1(c)]. In the case of untreated sample (bare Cu), lithium dendrite will be formed and penetrates through the SEI layer on the electrode. However, the PVDF-HFP@TiO$_2$ hybrid layer could induce uniform deposition without the growth of lithium dendrite due to its improved mechanical properties and ion conductivity [Scheme 1(d)][17].

3.2. Material characterization of PVDF-HFP@ TiO$_2$ hybrid membrane

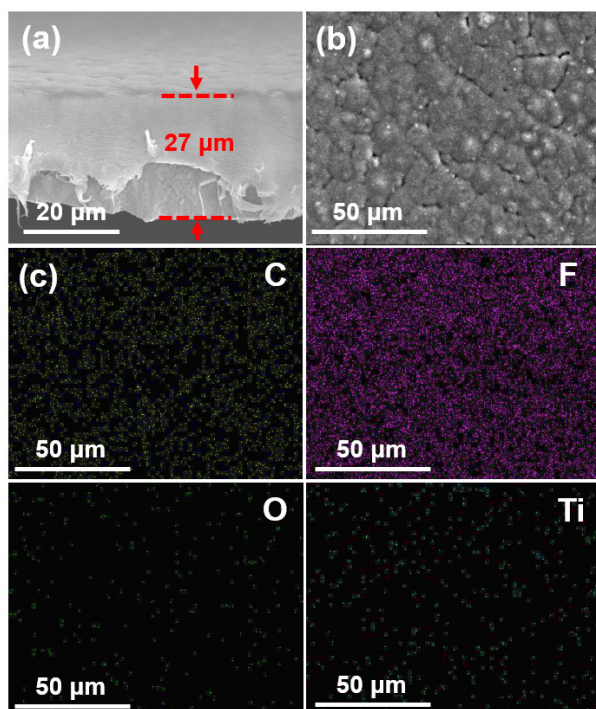Fig. 1(a) indicates the cross-section image of PVDF-HFP-

Fig. 1. SEM images of PVDF-HFP@TiO$_2$ hybrid membrane (a) cross section, (b) top view. (c) Elemental mapping of PVDF-HFP@TiO$_2$ hybrid [C (green), F (purple), O (white), Ti (cyan)].

Fig. 2. AFM images of PVDF-HFP@TiO$_2$ hybrid membrane (a) plane view (b) three dimensionally reconstructed image.

Fig. 3. XRD patterns of PVDF-HFP@TiO$_2$ hybrid membrane.

@TiO$_2$ hybrid membrane (TiO$_2$: 5 wt%) coated on a Cu electrode. The thickness of the membran represents 27 μm by SEM image [Fig. 1(a)]. Slight decrease of the film thickness occurred due to the evaporation of NMP solvent during drying process. Fig. 1(b) shows a top view of the PVDF-HFP@TiO$_2$ hybrid membrane. In the SEM image, TiO$_2$ nanoparticles are observed as white dots, which exhibits well dispersion of TiO$_2$ nanoparticles on the PVDF-HFP matrix. For more detailed analysis, the elemental mapping analysis was performed. As shown in Fig. 1(c), carbon and fluorine atoms from PVDF-HFP and small amounts of titanium and oxygen atoms from TiO$_2$ nanoparticles are observed. It indicates uniform distribution of TiO$_2$ nanoparticles and PVDF-HFP throughout hybrid layer.

Atomic force microscope (AFM) analysis was performed for in-detailed surface observation of the PVDF-HFP@TiO$_2$ hybrid membrane. Fig. 2(a) shows the morphology of PVDF-HFP@TiO$_2$ hybrid membrane.
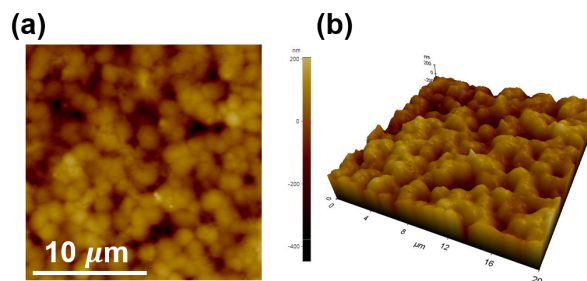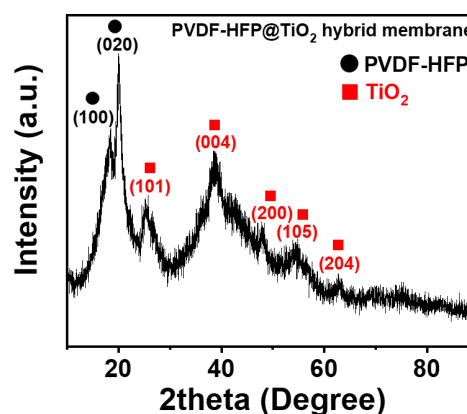
Empty spaces were generated by the evaporation of NMP, and it can be confirmed that the film coating was formed uniformly except for a few empty spaces. Fig. 2(b) shows the surface roughness of the PVDF-HFP-@TiO$_2$ hybrid membrane. Most of the coated films exhibit surface roughness below 100 nm, which refers this degree of surface roughness is negligible. From this data, it is confirmed that the PVDF-HFP@TiO$_2$ hybrid membrane is formed uniform surface. It can also referred that a few nanometers of TiO$_2$ nanoparticles would not have a significant effect on film surface roughness.

Fig. 3 indicates the X-ray diffraction (XRD) patterns of the PVDF-HFP@TiO$_2$ hybrid membrane. PVDF-HFP is known as a polymer having both amorphous and crystalline properties. The diffraction peaks of PVDF-HFP indicate (100) and (020) planes, and
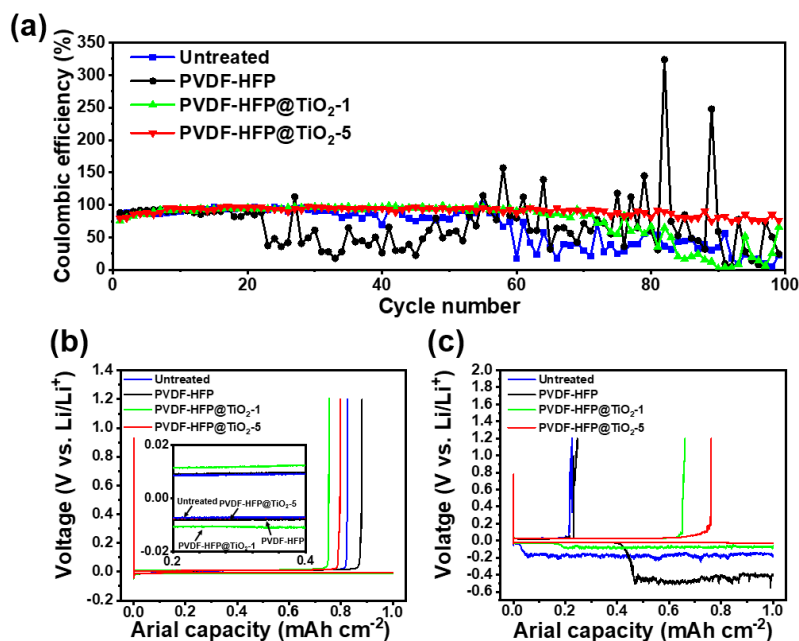
Fig. 4. Comparative electrochemical performance for Li|Cu half cell using protective layers (PVDF-HFP@TiO$_2$, TiO$_2$: 0~5 wt%.) on Li metal electrode (a) coulombic efficiencies at current density at 1 mA/cm^2; Voltage profiles of Li|Cu half cells measure at (b) first cycle, (c) 100th cycle.

peaks of TiO$_2$ anatase represent (101), (004), (200), (105), and (204) planes. From these results, the film prepared in this study is considered an polymer-inorganic composite of PVDF-HFP and TiO$_2$, it is expected that the lithium dendrite can be effectively suppressed and the improved lithium ion transport can be achieved by the addition of TiO$_2$[18,19].

3.3. Electrochemical analysis

Fig. 4(a) exhibits the coulombic efficiency of PVDF-HFP@TiO$_2$-5 (TiO$_2$: 5 wt%), PVDF@TiO$_2$-1 (TiO$_2$: 1 wt%), PVDF-HFP (TiO$_2$: 0 wt%), and untreated sample (bare Cu). Untreated sample shows stable coulombic efficiency until the 55th cycles, but it shows unstable coulombic efficiency in subsequent cycles. PVDF-HFP electrode retains stable coulombic efficiency until 20th cycles. Compared to the untreated sample and the PVDF-HFP, hybrid membrane indicated relatively stable coulombic efficiency. PVDF-HFP@-TiO$_2$-1 and PVDF-HFP@TiO$_2$-5 shows stable coulombic efficiency up to 70th cycles and up to 100th cycle, respectively. Fig. 4(b) represents the voltage profiles of

each samples in the first cycle. At the first cycle, lithium deposition/stripping voltage does not show significantly differences among PVDF-HFP@TiO$_2$-5, untreated sample, PVDF-HFP, and PVDF-HFP@TiO$_2$-1, except for a small difference of less than 2 mV. Fig. 4(c) represents the voltage profiles of the last cycle. As a result, PVDF-HFP@TiO$_2$-5 indicates low overpotential less than 20 mV, and PVDF-HFP@TiO$_2$-1 shows overpotential of 85 mV. Untreated sample and PVDF-HFP show very high overpotential of 200 and 500 mV, respectively. The detailed comparison of electrochemical performances between untreated sample and PVDF-HFP-@TiO$_2$-5 was shown in Fig. 5.

Fig. 5(a) represents the voltage-time curves of PVDF-HFP@TiO$_2$-5 and untreated sample, respectively. As the battery tests proceed, higher overpotential is observed in untreated sample while PVDF-HFP@TiO$_2$-5 shows stable overpotential from initial to later cycles. For a more detailed comparison, voltage-time curves of PVDF-HFP@TiO$_2$-5 and untreated sample at the initial and later cycles are shown in Fig. 5(b) and Fig. 5(c). Both samples indicate low overpotential at the initial
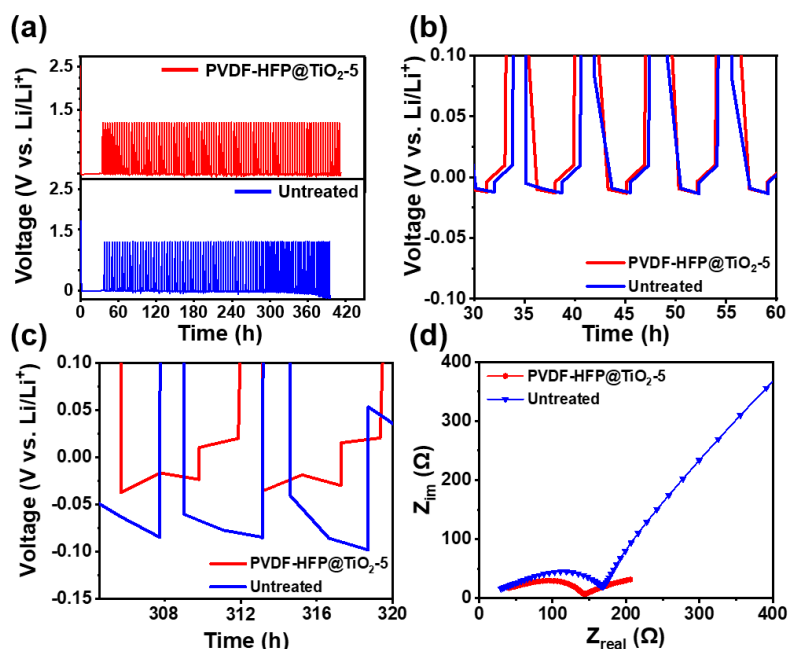
Fig. 5. (a) Voltage-time curves of PVDF-HFP@TiO$_2$-5/Cu and untreated sample at current density of 1 mA/cm^2. Enlargement of voltage-time curves at the (b) initial cycle and (c) 100th cycle. (d) EIS spectra of PVDF-HFP@TiO$_2$-5/ Cu and untreated sample before cycle.

cycle. However, in later cycles, PVDF-HFP@TiO$_2$-5 retains the initial overpotential well, while untreated sample exhibits much higher overpotential due to the growth of lithium dendirte, irreversibility of SEI layer and dead lithium. Fig. 5(d) shows the EIS spectra of PVDF-HFP@TiO$_2$-5 and untreated sample before cycle. The semicircles in the EIS spectra represent charge transfer (R$_{ct}$). The R$_{ct}$ value of PVDF-HFP@TiO$_2$-5 is smaller than untreated sample. This result is explained because of improved ion conductivity of PVDF-HFP-@TiO$_2$ hybrid membrane and the good compatibility with electrode and electrolyte. As a result, the PVDF-HFP@TiO$_2$-5 hybrid layer can effectively suppress the dendrite by its high mechanical strength, improved ion conductivity, and the compatibility of hybrid layer-electrode, hybrid layer-electrolyte[20,21].

4. Conclusion

In this study, the polymer-inorganic hybrid layer was designed as a protective layer for effective suppression of lithium dendrite on the electrode. PVDF-HFP was used as an polymer material and TiO$_2$ was used as an inorganic material. PVDF-HFP is a highly flexible polymer material that acts as the matrix of inorganic materials. TiO$_2$ used as an inorganic material which improves the mechanical strength and ion conductivity of the protective layer. From characterizations, it is found that the designed protective layer have the structure in which TiO$_2$ nanoparticles were evenly dispersed in the PVDF-HFP matrix. As a result of electrochemical analysis, untreated sample maintained stable coulombic efficiency until the 55th cycles, while PVDF-HFP@TiO$_2$ hybrid membrane showed high coulombic efficiency, 80% until the 100th cycles. Furthermore, from the voltage profiles and voltage-time curves, untreated sample represented the high overpotential of 200 mV in the last cycle, but PVDF-HFP@TiO$_2$ hybrid membrane maintained a low overpotential, less than 20 mV. These results indicate that lithium dendrite was effectively suppressed due to the high flexibility of PVDF-HFP matrix, the enhancement of ion conductivity and mechanical strength by addition of TiO$_2$.

Acknowledgements

Reference

1. H. Sohn, Q. Xiao, A. Seubsai, Y. Ye, J. Lee, H. Han, S. Park, G. Chen, and Y. Lu, "Thermally robust porous bimetallic (Ni_xPt_{1-x}) alloy particles within carbon framework: High-performance catalysts for hydrogenation reaction and oxygen reduction", *ACS Appl. Mater. Interfaces*, **11**, 21435 (2019).

2. D. Seok, Y. Jeong, K. Han, D. Y. Yoon, and H. Sohn, "Recent progress of electrochemical energy devices: Metal oxide-carbon nanocomposites as materials for next-generation chemical storage for renewable energy", *Sustainability*, **11**, 3694 (2019).

3. D. Seok, Y. Kim, and H. Sohn, "Synthesis of Fe_3O_4/porous carbon composite for efficient Cu^{2+} ions removal", *Membr. J.*, **29**, 308 (2019).

4. F. Dai, R. Yi, H. Yang, Y. Zhao, L. Luo, M. L. Gordin, H. Sohn, S. Chen, C. Wang, S. Zhang, and D. Wang, "Minimized volume expansion in hierarchical porous silicon upon lithiation", *ACS Appl. Mater. Interfaces*, **11**, 13257 (2019).

5. H. Sohn, D. H. Kim, R. Yi, D. Tang, S. E. Lee, Y. S. Jung, and D. Wang, "Semimicro-size agglomerate structured silicon-carbon composite as an anode material for high performance lithium-ion batteries", *J. Power Sources*, **334**, 128 (2016).

6. D. Y. Oh, Y. E. Choi, Y. G. Lee, J. N. Park, H. Sohn, and Y. S. Jung, "All-solid lithium-ion batteries with TiS_2 nanosheet and sulfide solid electrolytes", *J. Mater. Chem. A*, **4**, 10329 (2016).

7. D. Tang, Q. Huang, R. Yi, F. Dai, M. L. Gordin, S. Hu, S. Chen, Z. Yu, H. Sohn, J. Song, and D.

Wang, "Room-temperature synthesis of mesoporous Sn/SnO_2 composite as anode for sodium-ion batteries", *Euro. J. Inorg. Chem.*, **2016**, 1950 (2016).

8. H. Sohn, M. L. Gordin, M. Regula, D. H. Kim, Y. S. Jung, J. Song, and D. Wang, "Porous spherical polyacrylonitrile-carbon nanocomposite with high loading of sulfur Li-S batteries", *J. Power Sources*, **302**, 70 (2016).

9. Y. Gu, A. Wu, H. Sohn, C. Nicoletti, Z. Iqbal, and J. F. Federici, "Fabrication of rechargeable lithium-ion batteries using water-based inkjet printed cathodes", *J. Manufactur. Processes*, **20**, 198 (2015).

10. J. Song, M. L. Gordin, T. Xu, S. Chen, Z. Yu, H. Sohn, J. Lu, Y. Ren, Y. Duan, and D. Wagn, "Strong lithium polysulfide chemisorption on electroactive sites of nigrogen-doped carbon enables high-performance lithium-sulfur battery cathodes", *Angew. Chem. Int. Ed.*, **54**, 4325 (2015).

11. H. Sohn, M. L. Gordin, T. Xu, S. Chen, D. Lv, J. Song, A. Manivannan, and D. Wang, "Porous spherical carbon/sulfur nanocomposites by aerosol-assisted synthesis: The effect of pore structure and morphology on their electorchemical performance as lithium-sulfur battery cathodes", *ACS Appl. Mater. Interfaces*, **6**, 7596 (2014).

12. C. Lei, Z. Chen, H. Sohn, X. Wang, Z. Le, D. Wang, M. Shen, G. Wang, and Y. Lu, "Better lithium-ion storage materials made through hierarchical assemblies of active nanorods and nanocrystals", *J. Mater. Chem. A*, **2**, 17536 (2014).

13. B. Zhu, Y. Jin, X. Hu, Q. Zheng, S. Zhang, Q. Wang, and J. Zhu, "Poly (dimethylsiloxane) thin film as a stable interffacial layer for high-performance lithium-metal battery anodes", *Adv.*, **29**, 1603755 (2017).

14. H. Sohn, "Deposition of functional organic and inorganic layer on the cathode for the improved electrochemical performance of Li-S battery", *Korean Chem. Eng. Res.*, **55**, 483 (2017).

15. K. B. Hwang, H. Sohn, and S. H. Yoon, "Mesostructured niobium-doped titanium oxide-carbon

(Nb-TiO₂-C) composite as an anode for high-performance lithium-ion batteries", *J. Power Sources*, **378**, 225 (2018).

16. K. M. Kim, N. G. Park, K. S. Ryu, and S. H. Chang, "Characteristic of PVDF-HFP/TiO₂ composite membrane electrolytes prepared by phase inversion and conventional casting methods", *Electrochim. Acta*, **51**, 5636 (2006).

17. J. Lang, J. Song, L. Qi, Y. Luo, X. Luo, and H. Wu, "Uniform lithium deposition induced by polyacrylonitrile submicron fiber array for stable lithium metal anode", *ACS Appl. Mater. Interfaces*, **9**, 10360 (2017).

18. H. Sohn, D. Kim, J. Lee, and S. Yoon, "Facile synthesis of mesostructured TiO₂-graphitized carbon (TiO₂-gC) composite through the hydrothermal process and its application for the anode of lithium ion battery", *RSC Adv.*, **6**, 39484 (2016).

19. J. Wilson, G. Ravi, and M. A. Kulandainathan, "Electrochemical studies on inert filler incorporated poly (vinylidene fluoride-hexafluoropropylene) (PVDF-HFP) composite electroltyes", *Polimeros.*, **16**, 88 (2006).

20. X. B. Cheng, R. Zhang, C. Z. Zhang, and Q. Zhang, "Toward safe lithium metal anode in rechargeable batteries: A review", *Chem. Rev.*, **117**, 10403 (2017).

21. W. Xu, J. Wang, F. Ding, X. Chen, E. Nasybulin, Y. Zhang, and J. G. Zhang, "Lithium metal anodes for rechargeable batteries", *Energy Environ. Sci.*, **7**, 513 (2014).